Trackability of distal access catheters: a quantified evaluation of navigation strategies

Jiahui Li[1,2], Alejandro Tomasello[3], Manuel Requena[2,3], Oscar Castaño[4,5], David F Kallmes[6], Inyaki Galve[7], Pere Canals[1,2], Riccardo Tiberi[1,8], Elisabeth Engel[8,9], Marc Ribo[1,2]

1. Stroke Unit, Neurology, Vall d'Hebron University Hospital, Barcelona, Spain
2. Departament de Medicina, Universitat Autònoma de Barcelona, Barcelona, Spain
3. Neuroradiology, Vall d'Hebron University Hospital, Barcelona, Spain
4. Electronics and Biomedical Engineering, University of Barcelona, Barcelona, Spain
5. Biomaterials for Regenerative Therapies, Institute for Bioengineering in Catalonia, Barcelona, Spain
6. Radiology, Mayo Clinic, Rochester, Minnesota, USA
7. R&D, Anaconda Biomed SL, Barcelona, Spain
8. Materials Science and Engineering, Technical University of Catalonia, Barcelona, Spain
9. CIBER en Bioingeniería, Biomateriales y Nanomedicina, CIBER, Madrid, Spain

Corresponding author:

Marc Ribo

Stroke Unit, Neurology, Vall d'Hebron University Hospital, Barcelona, Spain

Hospital Vall d'Hebron, Passeig de la Vall d'Hebron Barcelona 119-129, Spain

E-mail: marcriboj@hotmail.com

Cover title: Navigability of distal access catheters

Keywords: Stroke treatment, trackability, thrombectomy catheters, in vitro testing

Word count: 3183

Tables: 1 **Figure:** 3

ABSTRACT

Background In mechanical thrombectomy (MT), distal access catheters (DACs) are tracked through the vascular anatomy to reach the occlusion site. The inability of DACs to reach the occlusion site has been reported as a predictor of unsuccessful recanalization. We aim to evaluate and provide an objective comparison among various DACs and navigation techniques.

Methods We designed an experimental setup to monitor DACs track forces when navigating in an *in vitro* anatomical model. Experiments were recorded to study mechanical behaviors such as tension buildup against vessel walls, DACs buckling, and abrupt advancements. A multiple regression analysis was performed to predict track forces from catheters' design specifications.

Results DACs were successfully delivered to the target M1 in 60 of 63 in vitro experiments (95.24 %). Compared to navigation with bare DAC, the concomitant use of a microcatheter with and without SR anchoring significantly reduced the track forces by about 80 % and 67 %, respectively ($p<0.01$). Our results showed high variability in devices' performance. We identified that combined coil and braid reinforcement configuration and a thinner distal wall are predictors of lower track force ($R^2 =0.758$; $p<0.001$).

Conclusions The use of microcatheter and SR facilitates smoother navigation of DACs through the vascular tortuosity to reach the occlusion site, which in turn could minimize vascular injuries and improve MT efficacy by increasing precision when positioning the DAC closer to the thrombus interface.

SUMMARY

Track force is a quantitative metric of devices' navigability. This study aims to provide insight into how to navigate devices through the vascular anatomy with minimal track forces, since higher forces may imply more risk of vascular injuries. The use of a stent-retriever as an anchor before advancing the distal access catheter stabilizes the catheter system and minimizes track forces to reach the M1 artery segment. Data reported may be helpful for the optimization of thrombectomy strategies.

INTRODUCTION

Mechanical thrombectomy (MT) is a widely performed procedure for acute ischemic stroke. Over the last decade, a variety of new devices and techniques have been developed to reduce the recanalization time and improve clinical outcomes [1], [2].

Distal access catheters (DACs) are used to perform direct aspiration or combined technique with a stent-retriever (SR). In both MT strategies, DACs are tracked through the vascular anatomy to reach the occlusion site. Previous studies reported that placing the distal tip of DACs adjacent to the thrombus before applying the combined technique [3] and maximizing the catheter-to-vessel diameter ratio [4], [5] allowed to achieve better reperfusion rates. However, the use of larger-bore DACs may imply more difficulty to access the intracranial segments, and advancing the devices through tortuous vessels may imply a higher risk of vascular injury.

The inability of DACs to navigate past the ophthalmic segment of ICA has been reported as a predictor of unsuccessful recanalization [6]. A navigation approach for challenging cases using the SR as an anchor has shown to be effective making possible to deliver the DACs to the target site. Briefly, the SR anchoring technique consists, first, in positioning a long sheath in the proximal ICA to advance the DAC as distally as possible. Then, a microcatheter is tracked further over a microwire to cross the occlusion site and lastly, a SR is deployed over the clot and used as an anchor to tension the wire and navigate the DAC closer to the proximal aspect of the thrombus.

Considering the improved clinical outcomes of placing large-bore DACs as close to the thrombus interface as possible while at the same time minimizing vessel wall damage during the MT procedure, this study proposes an *in vitro* testing platform capable of reproducing DACs navigation performance in clinical scenarios. In this work, we first report a clinical case of tension buildup-release and abrupt progression of DAC in a tight turn of the vascular anatomy. Second, we provide an objective comparison among various DACs and navigation techniques. Additionally, associations between device navigability and design specifications will be analyzed.

METHODS

The quantitative metric used in this study to evaluate navigability is the force (F) required to track through a vascular phantom [7], [8]. Since higher forces exerted against the vessel walls may imply more events of vascular injury, lower track forces are considered as an indicator of better trackability. The navigation

approaches to evaluate are 1) bare DACs with the proximal support of a guiding catheter (bare DAC); 2) DACs combined with microcatheter and microwire (DAC-mC), and 3) anchoring an SR before advancing the DACs to the target site (DAC-SR).

Materials & Equipment

The following DACs were included in this study: ACE 68 and JET 7 (Penumbra, Inc, CA, USA), React 68 and React 71 (Medtronic, MN, USA), Cat 6 and Vecta 74 (Stryker, MI, USA), and Sofia Plus (Microvention, CA, USA). DACs design specifications are detailed in **Table 1**. Neuron Max 088 long sheath (Penumbra, Inc, CA, USA) was the selected guiding catheter for all experiments. For the navigation with DAC-mC, Headway 21 microcatheter (Microvention, CA, USA) and Synchro 14 microwire (Stryker, MI, USA) were used. For the navigation with the DAC-SR anchor technique, Solitaire X 4 x 20 mm (Medtronic, MN, USA) was delivered through the Headway 21 microcatheter.

As for the *in vitro* anatomical model, we utilized a glass-made phantom (Farlow's Scientific Glassblowing, Inc., CA, USA) that reproduced a simplified version of the vascular anatomy from the right common carotid artery to the M1. The geometrical specifications of the glass phantom are detailed in **Supplementary Table 1.**

All experiments were performed with a Zwick-Roell Zwick-line Z0.5TN universal testing machine (Zwick-Roell, Ulm, Germany) equipped with a 10 N load cell and operating in compression mode controlled by testXpert II software (Zwick Roell Group Ltd., Ulm, DE).

Testing platform

We designed an experimental setup (**Figure 1**) to monitor DACs' track forces when navigating in a glass phantom. Silicone tubings were used to connect the phantom in the flow loop setting and to simulate the femoral artery with an 8 F sheath, through which Neuron Max 088 was introduced and positioned at the proximal internal carotid artery. Since the testing machine was vertically configured and the flow model was in a horizontal setup, we adjusted the angle to approximately 90 degrees to mimic the access from the aortic arch to the right carotid artery and simulate the mechanical constraints that DACs experience during the navigation. The flow loop setting was maintained at 37±1 ºC and distilled water was circulating at a physiological flow rate of 200 mL/min, which is an approximation of the blood supply at MCA territory [9].

Navigability experiments

For experiments of navigation with bare DAC, we introduced the selected DAC 96 cm into the guiding catheter and attached it to the force sensor at 110 cm from its distal end. The initial position of the DAC was adjusted so the distal end was 13 cm below the distal M1 segment of the MCA. The guiding catheter's proximal end was fixed before starting each experiment. Once that catheters' setting was prepared, the motor-driven force sensor started to advance at 1 cm/s to navigate the DAC through the flow model.

Regarding the test setting for the DAC-mC technique, a microcatheter and a microwire were positioned at the level of the targeted M1, then the microcatheter's proximal end was subjected while DACs were tracked over the support. Similarly, for the DAC-SR approach, a SR was delivered along with the microcatheter to distal M1, where the deployed SR exerted radial force on the vascular walls, and then the SR wire was held in tension by pulling and fixing the SR wire's proximal end before starting each experiment. The tension applied to the SR wire was just enough to keep the wire as straight as possible without retraction of the SR from the original deployment site.

Each set of experiments per DAC was replicated 3 times with brand new devices (N=3). A total of 63 experiments were conducted (7 DACs x 3 techniques x 3 replications per combination). Videos of the experiments were recorded for each device and navigation approach combination. An experiment was considered successful if the DAC could complete the 13 cm trajectory and reach the distal M1 segment of MCA.

To measure the differences in the progressed distance between DACs proximal and distal end (ΔD), graph paper was utilized as a reference background, and frames from videos recordings were analyzed using ImageJ (U.S. National Institutes of Health, Maryland, USA). In case DAC's proximal and distal end advancement was 1:1 proportional at all times, max-ΔD=0. By contrast, if the DAC's proximal end was moving forward while the distal end was still or advancing slower due to the vessel tortuosity, max-ΔD>0.

The forces required to navigate through the vascular curves were continuously recorded to obtain the proximal track force vs. DAC proximal displacement graphics (**Figure 2**). The comparative analysis was focused on the forces required to pass the curvatures in the petro-cavernous (trajectory D-E) and ophthalmic (trajectory F-G) segments of ICA. Cumulative track forces were calculated by adding forces required for both trajectories.

Clinical case

An illustrative clinical case of a sudden progression of the DAC's distal tip was recorded during a MT procedure and reported as **Supplementary Video 1.**

Statistics

Track forces and max-ΔD were presented as mean ± standard deviation. One-way ANOVA and Tukey's HSD post hoc analysis were used to assess statistical differences between navigation techniques and DACs, $p<0.05$ was considered statistically significant.

A hierarchical multiple regression analysis was performed to predict cumulative track forces from DACs' geometrical specifications (ID, OD, and wall thickness at the distal end), reinforcement material (nitinol vs. stainless steel), and configuration (coil vs. hybrid coil + braid). Pearson's correlation tests were performed to assess linearity and multicollinearity and select which variables should be included in the regression model. To determine whether independent variables added statistical significance to the prediction, $p<0.05$ was considered.

All statistical tests were performed using SPSS Statistics (IBM Corp., NY, USA)

RESULTS

Clinical case

Supplementary Video 1 shows an MT procedure where React 71 was advanced over Headway 21 and Synchro 14 microwire into the M1 branch, where the following sequence of events occurred: DAC's tip wedging against the vessel wall, tension buildup that led to the proximal displacement of the guiding catheter and subsequent tension release that resulted in an abrupt advancement of DAC's distal end to the proximal aspect of the thrombus.

In vitro testing

DACs were successfully delivered to the target M1 in 60 of 63 in vitro experiments (95.24 %). All tested DACs could reach the target M1 using either of the three navigation techniques, except for ACE 68, in which case DAC alone could not reach the target site and DAC-mC or DAC-SR was necessary. The measured track forces and max-ΔD for each device-navigation strategy combination are reported in **Supplementary Tables 2-5**.

We observed that when navigating with DAC alone in the glass phantom (**Supplementary Videos 2-3**), all DACs stopped momentarily at the turn in the petro-cavernous segment of ICA despite the constant advancement of DAC's proximal end. As the DACs' tip wedged against the vessel wall and accumulated tension to keep advancing, the vessel wall was exerting the same amount of normal force on the devices and multiple parts of DACs' distal section began to buckle until the DACs' tip were deflected. Immediately after the tip deflection, a tension release occurred and the DACs distal end advanced abruptly from the petro-cavernous to the ophthalmic segment of ICA, where, once again, the devices' tip edge collided against the vessel wall to start a gradual force buildup and buckling to cross the curve. During the buckling, the guiding catheter experienced a proximal displacement of 3-5 mm despite being subjected at its proximal end. Moreover, we identified that this buckling behavior resulted in max-ΔD up to 2.3 cm.

In contrast to bare DAC, when using the DAC-mC or DAC-SR techniques (**Supplementary Videos 4-5**), all DACs passed the petro-cavernous segment's turn smoothly without significantly wedging against the vessel walls. Nevertheless, tension accumulation to pass the ophthalmic segment of the ICA was needed anyway and guiding catheter displacements were observed in many DAC-mC experiments. Max-ΔD using either DAC-mC or DAC-SR were significantly lower than navigation with bare DAC ($p<0.05$).

Specific proximal track force vs. DAC proximal advancement graphics for each device-technique combination are presented in **Supplementary Figures 1-7.** The use of DAC-mC and DAC-SR suppressed the sharpest force peak during the trajectory through the petro-cavernous segment of the ICA.

Trajectory through the petro-cavernous segment

When navigating with the bare DAC approach, track forces in the DAC's trajectory through the petro-cavernous segment of ICA ranged from 540 to 1500 mN. Amongst all DACs, Sofia Plus required the lowest track forces to cross the curve ($F = 561.19 \pm 22.95$ mN; $p<0.01$). No significant peaks were recorded at this level when using DAC-mC or DAC-SR techniques.

Trajectory through the ophthalmic segment

Overall, DAC-SR required significantly lower mean track forces ($F = 306.72 \pm 143.93$ mN) and experienced less ΔD (max-ΔD = 0.27 ± 0.26 cm) than DAC-mC ($F = 517.62 \pm 320.91$ mN; max-ΔD = 0.54 ± 0.15 cm) and bare DAC ($F = 690.08 \pm 225.36$ mN; max-ΔD = 0.98 ± 0.55 cm). In all cases, $p<0.05$. However, the mean difference in track forces between bare DAC and DAC-mC was not significant, $p=0.061$.

When studying the devices' performance with the DAC-mC approach, the lowest track forces were measured for Cat 6 (262.46 ± 3.45 mN), Sofia Plus (285.89 ± 14.01 mN) and React 71 (299.08 ± 10.79 mN), without significant differences between them. Similarly, when using DAC-SR, React 71 (147.77 ± 4.98 mN) and Sofia Plus (195.20 ± 10.64 mN) required significantly less track force than other DACs.

Cumulative track forces

Cumulative track forces measured from the petrous to the ophthalmic segment of ICA using different DACs and navigation strategy combinations are shown in **Figure 3A-B**. Both DAC-mC and DAC-SR required significantly lower forces than the bare DAC approach, $p<0.01$. As compared to bare DAC, the mean track force decreased by 1047.38 mN when using DAC-mC and by 1258.27 mN when using DAC-SR. On the other side, the mean force reduction of 210.90 mN between DAC-mC and DAC-SR was not statistically significant, $p=0.079$.

Catheter design & navigability

Distal ID, OD, and reinforcement materials were not linearly related to cumulative track forces. DACs distal wall thickness only correlated to track forces in the bare DAC experiments ($r=0.49$; $p<0.05$). Thus, reinforcement configuration was included in all regression models and DACs distal wall thickness was only added to the model for the bare DAC approach.

The reinforcement configuration (coil vs. hybrid coil + braid) significantly explained 25.6%, 28.1%, and 41.4% of the total variance (R square) in track forces required to navigate with bare DAC, DAC-mC, and DAC-SR techniques, respectively. The presence of the braid pattern in the reinforcement significantly diminished the track forces, in all cases $p<0.05$ (Figure 3C).

DACs distal wall thickness and reinforcement configuration significantly predicted cumulative track forces in bare DAC experiments (F-value $(2,18) = 28.26$, $p<0.001$). The total variance explained by the model was 75.8% (R square change =0.503). Track forces decreased with hybrid reinforcement configuration and thinner walls at the distal end. The overall multiple correlation coefficient was $r=0.871$.

Figure 3C depicts the correlation between DACs distal wall thickness and cumulative forces from the bare DAC experiments. Beyond overall tendency, two trends can be distinguished according to devices' reinforcement configuration. For similar wall thicknesses, devices with combined coil and braid patterns presented significantly lower track forces.

DISCUSSION

In this benchtop study, we accurately recreated the clinical behavior of DACs traversing tortuous distal territories and showed quantifiable differences among navigation strategies and DACs that likely correlate directly with findings in clinical practice [6], [10].

Our results show high variability in devices' navigability. We identified that hybrid coil and braid reinforcement configuration and DACs' distal wall thickness are significant contributory factors to ease navigation. This is probably due to the braid structure that enhances the devices' pushability (force transmission from proximal to distal end), and thinner catheter walls that increase DAC distal end's flexibility. Nevertheless, these parameters did not fully explain the variance in track forces. Other design factors conditioning the navigability could be the reinforcement wire size, the braiding angle, the coil pitch, and the hydrophilic coating. On the other side, distal ID and OD were not associated with track forces, which suggests that larger-bore DACs are not necessarily less trackable.

DACs' performance varied depending on the selected navigation strategy, and the use of a microcatheter and SR bridged the gap between devices. No association was found between any catheters' geometrical feature and track forces measured from DAC-mC and DAC-SR experiments. This may be due to the presence of the microcatheter and SR that acted as a rail to keep the DACs tip aligned with the vessel centerline, minimizing the contact between DACs and vessel wall.

As our data suggest, DAC-mC and DAC-SR techniques provide stability to the catheter setting, which, along with the proximal support of the guiding catheter, facilitates a smooth advance of the DAC to the proximal aspect of the thrombus. In comparison to the bare DAC approach, cumulative track forces were reduced by about 67 % and 80 % (> 1000 mN) when using a microcatheter and SR anchoring, respectively. Considering ~100 mN as the reference of force discrimination ability [11], interventionalists may be able to sense differences in the buildup of tension when using DAC-mC versus DAC-SR, despite that mean difference between these navigation strategies (~200 mN) was not statistically significant.

Additionally, apart from the track force as a quantitative metric of this study, we could visually identify experiments where the guiding catheter experienced a slight proximal displacement (~4 mm) due to the tension accumulation against the vessel wall. That occurred mainly in bare DAC and DAC-mC experiments, which indicates that the DAC-SR anchoring technique further stabilized the catheter setting. In clinical practice, the observed displacement of the guiding catheter may have a deleterious effect in those patients

with a tortuous aortic arch. In these cases, where the guiding catheter is particularly unstable in the ICA, slight displacement may lead to the whole system falling in the aortic arch.

Discrepancies between DAC proximal and distal end advancement were observed in all experiments at the petro-cavernous and ophthalmic segments of the ICA. Once the DAC's distal tip realigns with the vessel's centerline, the tension release may lead to an abrupt progression in the absence of significant curvature in the immediately distal segment, such as the petro-cavernous segment (cumulative curvature = 0.42 mm^{-1}; segment's curvature = 0.17 mm^{-1}). However, the tension release does not necessarily lead to abrupt advancements, if further curves dampen the tension release, such as at the ophthalmic segment (cumulative curvature = 0.85 mm^{-1}; segment's curvature = 0.26 mm^{-1}). Thus, we hypothesize that the occurrence of sudden progression varies depending on cumulative curvatures in anatomy, and this behavior may be scarcer in highly tortuous anatomy in which the sudden progression may be buffered by the adjacent distal curves. Further investigation is warranted to evaluate the potential harm of such abrupt tension release on different anatomies with varying tortuosity degrees.

In line with a previous study [12], we did not find a clear association between curvature in a specific anatomical point and track forces. Focusing on the experiments with bare DAC settings, some DACs needed lower forces to overcome the turn at the ophthalmic segment than at the petro-cavernous ICA curve. This may partly be due to residual inertia from the sudden progression, but again, this suggests that the combination of curvatures in anatomy rather than the local isolated curvature defines the track forces required for navigation. Thus, it is possible that in a different anatomy or curves combination the relative performance of the different devices might be different, meaning that this particular anatomy may favor some devices and impair others.

Limitations

To better visualize the behavior of DACs in the anatomical model, we performed all experiments in a glass phantom, which could not reproduce the frictional and elastic properties of human arteries. Since the navigation to the target site is easier than in stroke patients [13] because of the lower friction, null vessel wall elastic response, and impossible vessel damage, the measured track forces may be an underestimation of forces required in clinical scenarios. Consequently, the relative movement of the guiding catheter during DAC advancement and max-ΔD may be underestimated as well. Lastly, different devices' relative performance may vary in different anatomy with other morphological variations and curvature combinations.

CONCLUSIONS

The SR anchoring technique diminishes the frequency of undesirable events during MT, such as a tension buildup against vessel walls, guiding catheter falling back down in the aortic arch, and abrupt progressions of DACs distal end. The use of microcatheter and SR facilitates smoother navigation of DACs through the vascular tortuosity to reach the occlusion site, which in turn could minimize vascular injuries and improve the MT efficacy by positioning the DAC closer to the thrombus interface.

Funding

Contributors

JL, MRi, AT, and OC conceived of the study and experimental setup design. JL, PC, and RT performed the experiments and statistical analyses. MRi and MRe reported the clinical case. JL and MRi drafted the manuscript. The article was critically revised by JL, MRi, MRe, DFK, IG, and EE. All authors approved the final version of the manuscript.

Competing interests

Patient consent for publication

Not required.

Data availability statement

Data relevant to the study are included in the article. All data are available upon reasonable request to the corresponding author.

References

[1] A. M. Spiotta, M. I. Chaudry, F. K. Hui, R. D. Turner, R. T. Kellogg, and A. S. Turk, "Evolution of thrombectomy approaches and devices for acute stroke: A technical review," *J. Neurointerv. Surg.*, vol. 7, no. 1, pp. 2–7, 2015, doi: 10.1136/neurintsurg-2013-011022.

[2] P. Bhogal, T. Andersson, V. Maus, A. Mpotsaris, and L. Yeo, "Mechanical Thrombectomy—A Brief Review of a Revolutionary new Treatment for Thromboembolic Stroke," *Clin. Neuroradiol.*, vol. 28, no. 3, pp. 313–326, 2018, doi: 10.1007/s00062-018-0692-2.

[3] S. Hun *et al.*, "Effect of distal access catheter tip position on angiographic and clinical outcomes following thrombectomy using the combined stent- retriever and aspiration approach," pp. 1–15, 2021, doi: 10.1371/journal.pone.0252641.

[4] A. A. Kyselyova, J. Fiehler, H. Leischner, F. Flottmann, J. H. Buhk, and A. M. Frölich, "Vessel diameter and catheter-to-vessel ratio affect the success rate of clot aspiration," *J. Neurointerv. Surg.*, vol. 13, no. 7, pp. 605–608, 2021, doi: 10.1136/neurintsurg-2020-016459.

[5] R. G. Nogueira, D. Ryan, L. Mullins, J. Thornton, and S. Fitzgerald, "Maximizing the catheter-to-vessel size optimizes distal flow control resulting in improved revascularization in vitro for aspiration thrombectomy," *J. Neurointerv. Surg.*, no. Id, pp. 184–188, 2021, doi: 10.1136/neurintsurg-2021-017316.

[6] J. Singh, S. Q. Wolfe, R. M. Janjua, and H. Hedayat, "Anchor technique : Use of stent retrievers as an anchor to advance thrombectomy catheters in internal carotid artery occlusions," 2015, doi: 10.1177/1591019915609170.

[7] M. Mokin *et al.*, "Assessment of distal access catheter performance during neuroendovascular procedures: Measuring force in three-dimensional patient specific phantoms," *J. Neurointerv. Surg.*, vol. 11, no. 6, pp. 619–623, 2019, doi: 10.1136/neurintsurg-2018-014468.

[8] B. T. Jankowitz, M. Shayan, A. M. Robertson, and Y. Chun, "In vitro assessment of the trackability of neurovascular intermediate catheters: A comparative analysis," *J. Med. Eng. Technol.*, vol. 38, no. 8, pp. 379–384, 2014, doi: 10.3109/03091902.2014.937833.

[9] L. Zarrinkoob, K. Ambarki, A. Wåhlin, R. Birgander, A. Eklund, and J. Malm, "Blood Flow Distribution in Cerebral Arteries," *J. Cereb. Blood Flow Metab.*, vol. 35, no. 4, pp. 648–654, Apr. 2015, doi:

10.1038/jcbfm.2014.241.

[10] J. J. Heit *et al.*, “Sofia intermediate catheter and the SNAKE technique: Safety and efficacy of the Sofia catheter without guidewire or microcatheter construct,” *J. Neurointerv. Surg.*, vol. 10, no. 4, pp. 401–405, 2018, doi: 10.1136/neurintsurg-2017-013256.

[11] W. Boisseau *et al.*, “Direct aspiration stroke thrombectomy: A comprehensive review,” *J. Neurointerv. Surg.*, vol. 12, no. 11, pp. 1099–1106, 2020, doi: 10.1136/neurintsurg-2019-015508.

[12] R. Finn and L. Morris, “An experimental assessment of catheter trackability forces with tortuosity parameters along patient-specific coronary phantoms,” *Proc. Inst. Mech. Eng. Part H J. Eng. Med.*, vol. 230, no. 2, pp. 153–165, 2016, doi: 10.1177/0954411915623815.

[13] Y. Liu *et al.*, “Preclinical testing platforms for mechanical thrombectomy in stroke: A review on phantoms, in-vivo animal, and cadaveric models,” *J. Neurointerv. Surg.*, vol. 13, no. 9, pp. 816–822, 2021, doi: 10.1136/neurintsurg-2020-017133.

Table 1. Distal access catheters' design parameters specified by devices' manufacturers.

SS: stainless steel; NiTi: nitinol; Hybrid: coil + braid.

Device	Distal ID (in)	Distal OD (in)	Distal wall thickness (in)	Reinforcement material	Reinforcement configuration
JET 7	0.072	0.085	0.00650	SS + NiTi	Coil
React 71	0.071	0.0855	0.00725	NiTi	Hybrid
ACE 68	0.068	0.084	0.00800	SS + NiTi	Coil
Cat 6	0.060	0.0709	0.00545	SS + NiTi + Polymer fiber	Coil
Sofia Plus	0.070	0.082	0.00600	SS	Hybrid
React 68	0.068	0.083	0.00750	NiTi	Hybrid
Vecta 74	0.074	0.083	0.00450	SS + NiTi	Coil

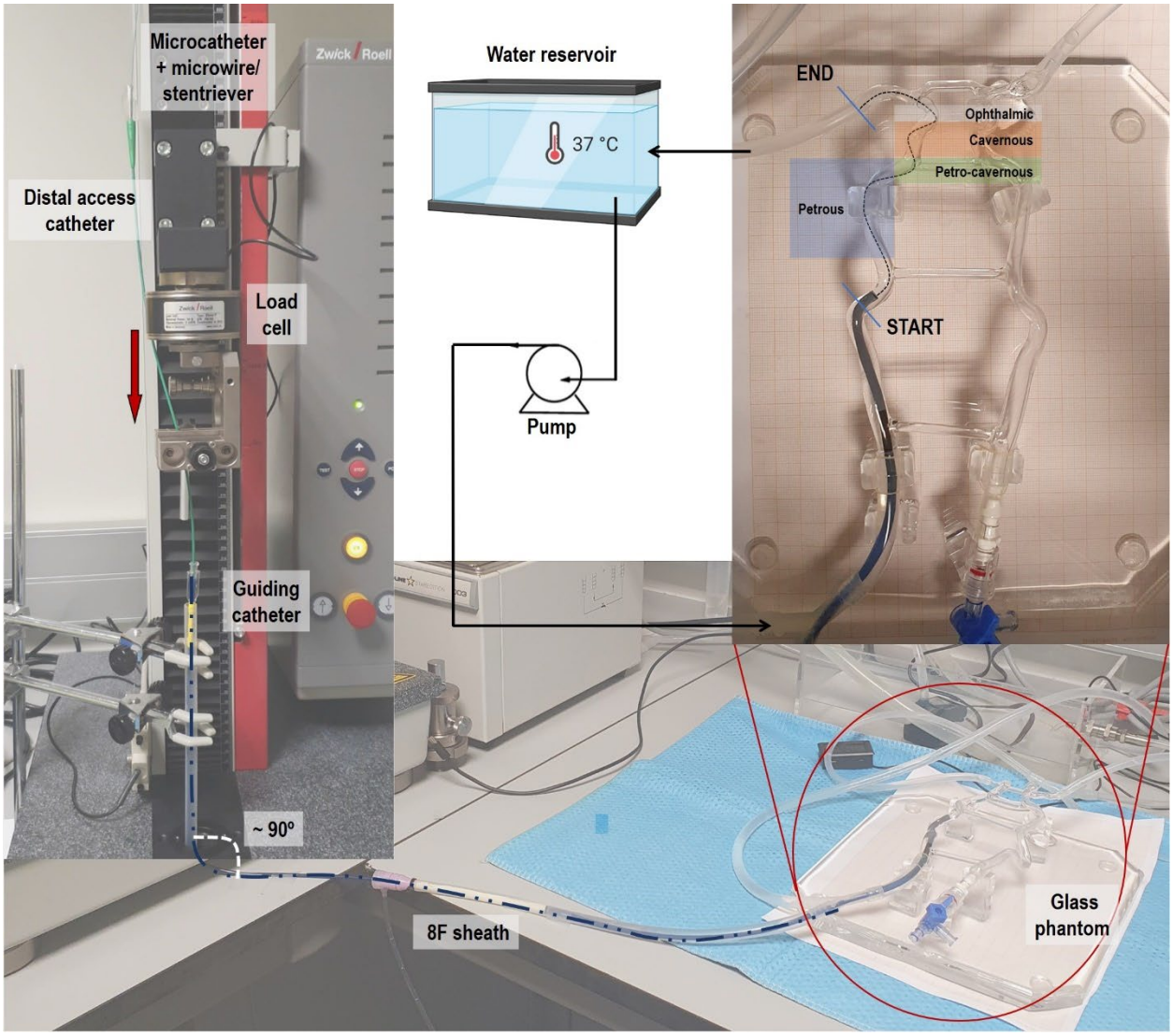

Figure 1. Experimental setup to monitor track forces of various navigation techniques and DACs.

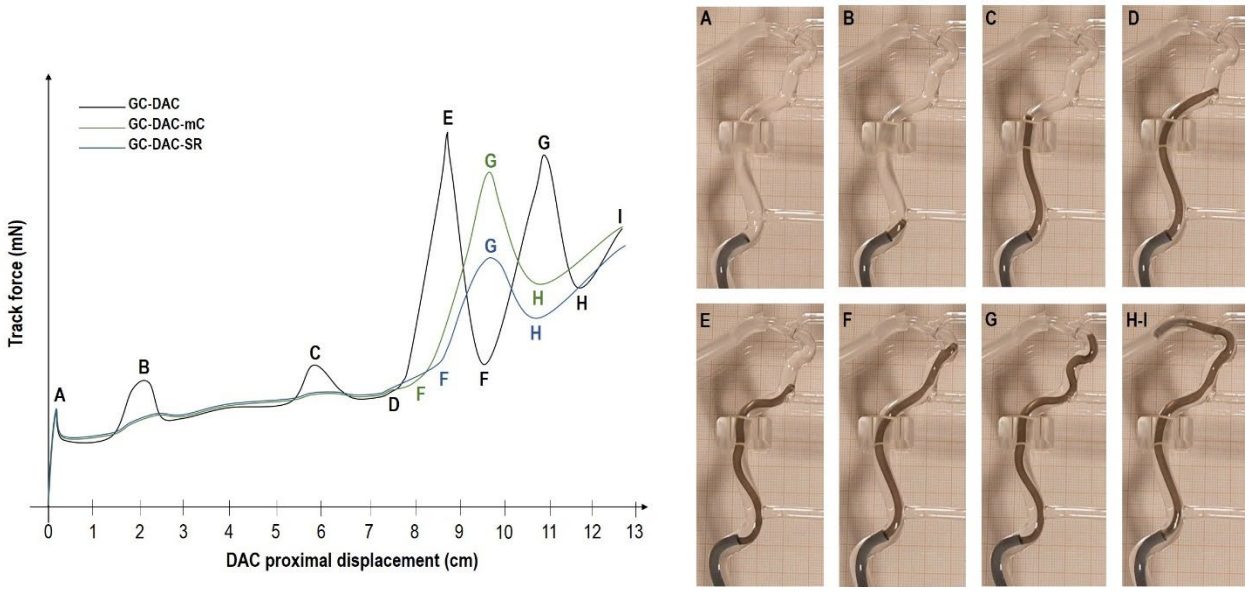

Figure 2. Generic track force vs. DAC proximal displacement graphics of different navigation approaches. A) Initial force to overcome the static friction resistance between DAC and guiding catheter. B) and C) track forces required to overcome the curvatures at 2 and 6 cm of the trajectory, respectively. D) Impact of DAC tip edge against the vessel wall, tension buildup, and beginning of DAC buckling at multiple points of the distal end. E) Frame right before the tension release and sudden progression of the DAC; the axial load on the distal part of the DAC deflected its tip before passing the vascular curve. F) Impact of the DAC against the vessel wall and beginning of tension buildup to pass the ophthalmic segment of ICA. G-H) DAC tip deflection and tension release without sudden progression. I) track force required to reach the end of the trajectory at M1.

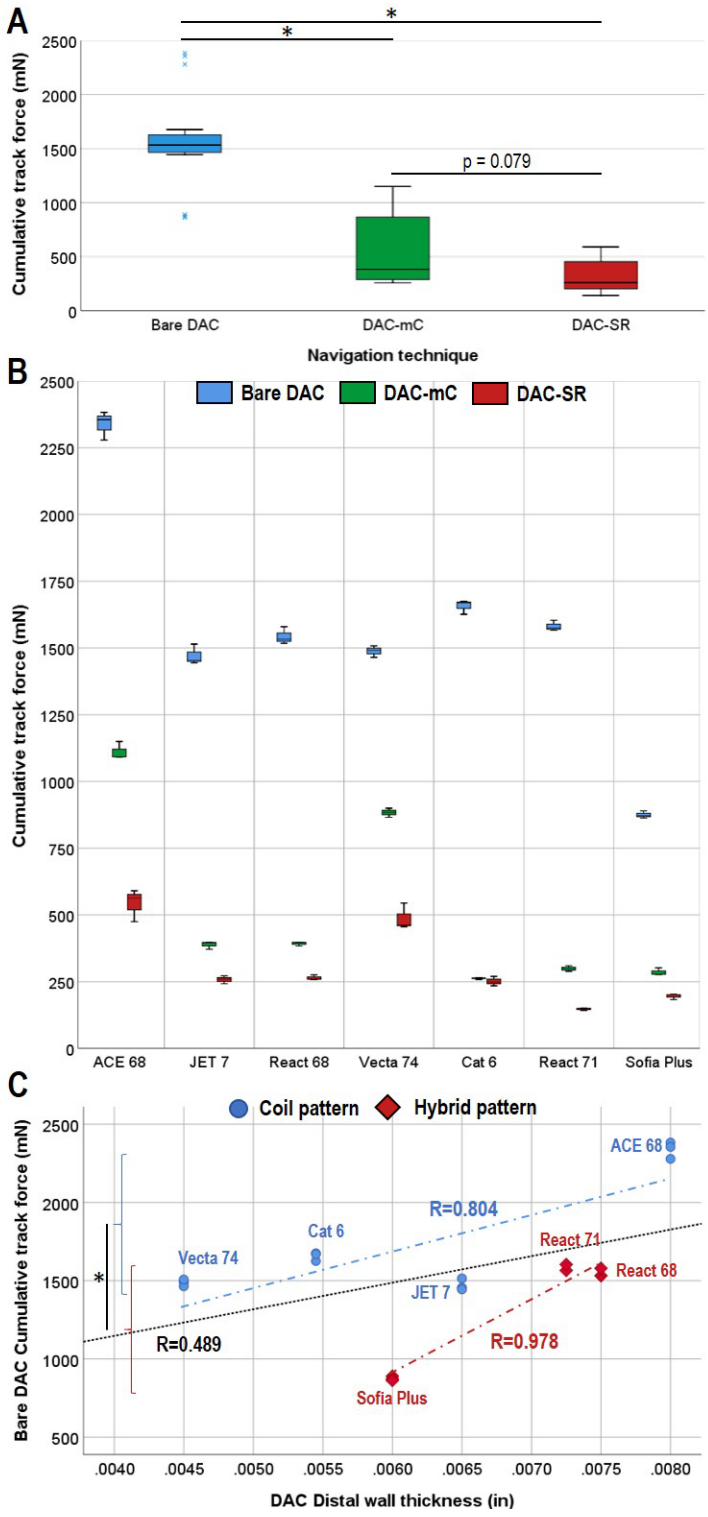

Figure 3. Cumulative track forces for A) different navigation techniques grouping all devices, and B) specific device-navigation strategy combinations (p-values in Supplementary Tables 3-5). C) Correlation between track forces in bare DAC navigation and distal wall thickness. Beyond the overall tendency (black) two trends (red and blue) can be discerned according to devices' reinforcement configuration.